Superconductivity in $Ba_{1-x}K_xBiO_3$

Wei Jin
Concurrent Computing Laboratory for Materials Simulations and Department of Physics and Astronomy, Louisiana State University, Baton Rouge, Louisiana 70803-4001 and Materials Science Division, Argonne National Laboratory, Argonne, Illinois 60439

Marcos H. Degani*
Materials Science Division, Argonne National Laboratory, Argonne, Illinois 60439

Rajiv K. Kalia and P. Vashishta
Concurrent Computing Laboratory for Materials Simulations and Department of Physics and Astronomy, Louisiana State University, Baton Rouge, Louisiana 70803-4001

(Received 17 July 1991; revised manuscript received 12 November 1991)

Superconductivity in $Ba_{1-x}K_xBiO_3$ is studied within the framework of Eliashberg theory using a model of the electron-phonon interaction, $\alpha^2F(\omega)$. The model is based upon molecular-dynamics calculations of the phonon density of states, which are in good agreement with inelastic-neutron-scattering experiments. The function $\alpha(\omega)$ is constructed using information from electron-tunneling experiments. Our model is constructed with the premise that the electron-phonon coupling constant $\lambda \approx 1$ and that strong electron-phonon coupling exists for high-energy (30–60 meV) phonon modes. Superconducting properties of the material at zero and finite temperatures are calculated and compared with experiments.

I. INTRODUCTION

$Ba_{1-x}K_xBiO_3$, for $x \sim 0.4$, exhibits superconductivity at $T_c \sim 30$ K, which is the highest transition temperature reported for any oxide material not containing copper.[1–14] Superconductivity in potassium-doped $BaBiO_3$ was discovered by Mattheiss, Gyorgy, and Johnson[1] in 1988, and the structure of the superconducting material was determined by Cava *et al.*[2] Hinks *et al.*[8–10] gave a detailed account of synthesis, structure, and transition temperature as a function of x. This discovery[1–14] of high-temperature superconductivity in the $Ba_{1-x}K_xBiO_3$ system has added a further interest because of the difference in the properties of this material and other copper-based layered oxides.[15,16] The most striking structural feature of these potassium-doped compounds is the absence of two-dimensional, metal-oxygen planes, which are widely believed to be an essential factor in producing a high transition temperature in the copper oxide system. This is because $Ba_{1-x}K_xBiO_3$ in the superconducting phase has a cubic perovskite structure of symmetry, $Pm\bar{3}m$ (Fig. 1). According to neutron-diffraction measurements,[17–19] potassium atoms are randomly distributed over the barium sites. The Bi-O-Bi bonds in the potassium-doped system form an orthorhombic or a simple cubic perovskite structure (depending on x), with each bismuth atom surrounded by six neighboring oxygen atoms.[17–19] Unlike other high-T_c copper oxide materials,[15] this material has no transition-metal atoms. In addition, local magnetic moments do not exist in these materials. They are diamagnetic.[5,20,21] The undoped compound $BaBiO_3$ is also diamagnetic and has a body-centered monoclinic ($I2/m$) structure.[19]

A wide range of experimental[17–60] and theoretical[61–78] investigations have been carried out on this material. Structural properties, electric, magnetic, thermal, and optical responses of the $Ba_{1-x}K_xBiO_3$ system have been studied. Infrared-reflectivity,[22–24] Raman-scattering,[25] inelastic-neutron-scattering,[26–28] electron-tunneling,[29–36] electron-diffraction,[37] photoemission, and inverse-photoemission[38,39] measurements have been carried out. The oxygen isotope effect,[3,20,42] specific heat[43,44,46] upper and lower critical magnetic fields,[3,47–49] thermal conductivity,[50] and thermoelectric power[20,51] have also been measured. Pei *et al.*[19] have investigated the crystalline structures for the entire composition range ($x = 0.0$–0.5) of this material by neutron powder diffraction, and the phase diagram as a function of temperature and composition has been determined. Coefficients of the Hall and Seebeck effects are determined[20,40] to be negative, indicating that the charge carriers are electrons, not holes.

A large isotope effect has been observed in T_c in the $Ba_{1-x}K_xBiO_3$ system. Batlogg *et al.*[3] measured the oxygen (^{16}O,^{18}O) isotope effect and found an exponent $\alpha_O = 0.22 \pm 0.03$ in the $T_c \sim M_O^{-\alpha_O}$ relation, where M_O is the mass of the oxygen isotope. Hinks *et al.*[42] have also measured the isotope effect for the $Ba_{0.625}K_{0.375}BiO_3$ system. Their dc resistivity and ac susceptibility measurements show that the substitution of ^{16}O by ^{18}O produces a shift of $\Delta T_c = 1.35 \pm 0.05$ K, leading to an isotope-effect exponent $\alpha_O = 0.41 \pm 0.03$. Kondoh *et al.*[20] also find a large isotope-effect exponent $\alpha_O = 0.35 \pm 0.05$ in $Ba_{1-x}K_xBiO_3$. This value is larger than the isotope-effect exponents in high-T_c cuprate superconductors. However, the isotope effect in these layered oxides remains controversial.[79]

 ©1992 The American Physical Society

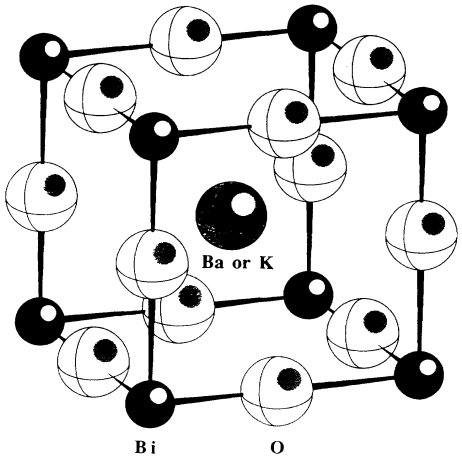

FIG. 1. Crystal structure of the cubic superconductor $Ba_{0.6}K_{0.4}BiO_3$.

High-energy optical-phonon modes have been observed in the phonon density of states (DOS). Recent inelastic-neutron-scattering measurements[26] of the generalized phonon DOS in the insulating $BaBiO_3$ and doped $Ba_{0.6}K_{0.4}BiO_3$ systems revealed three broadbands centered around 15, 35, and 61 meV. Molecular-dynamics (MD) simulations[26,80–82] showed that phonons of energy above 20 meV are due to oxygen vibrations. Softening of ~ 5 meV of oxygen phonons in the potassium-doped system relative to the undoped $BaBiO_3$ has been observed. The phonon spectra of ^{18}O and ^{16}O materials of $Ba_{0.6}K_{0.4}BiO_3$ are similar, except that phonons of energy larger than 20 meV in the ^{18}O material are shifted to lower values by 3–5 meV. These phonon peaks have also been observed in infrared[22] and Raman[25] measurements. Using inelastic-neutron-scattering measurements of the generalized phonon density of states, Loong *et al.*[27] have measured the reference isotope-effect exponent α_{Or} from the relation $\langle\omega\rangle \sim M_O^{-\alpha_{Or}}$, where $\langle\omega\rangle$ is the first frequency moment of the phonon DOS. Their value of the reference isotope-effect exponent, $\alpha_{Or}=0.42\pm0.05$, is close to $\alpha_O=0.41\pm0.03$ determined from T_c measurements by Hinks *et al.*[42]

Tunneling spectroscopy has indicated the contribution of relatively high-energy phonons in the $Ba_{1-x}K_xBiO_3$ system. Electron-tunneling measurements on polycrystalline $Ba_{1-x}K_xBiO_3$ by Zasadzinski *et al.*[29,30] revealed well-resolved structures in the high-energy range 30–60 meV. There is good agreement between the observed structures in the second derivative of the tunneling current and the positions of peaks in the phonon DOS from MD simulations[26,80] and inelastic-neutron-scattering experiments.[26] Since the size of the deviation of the normalized tunneling conductance from the weak-coupling BCS value scales roughly with the electron-phonon coupling constant λ, Zasadzinski *et al.* have estimated from the tunneling data that $\lambda \approx 1$. In a recent tunneling experiment on thin films of $Ba_{0.6}K_{0.4}BiO_3$, Sato, Takagi, and Uchida[31] find the ratio $2\Delta_0(0)/k_BT_c=3.7\pm0.5$, where $\Delta_0(0)$ is the superconducting energy gap at zero temperature. Using point-contact junctions, Huang *et al.*[33] have recently carried out electron-tunneling experiments on $Ba_{1-x}K_xBiO_3$ and $Nd_{2-x}Ce_xCuO_{4-y}$. They observe clear evidence of phonon images in the tunneling conductance up to 60 meV. Their quality of experimental data is sufficiently good that it has been possible to obtain the Eliashberg functions $\alpha^2F(\omega)$ for these materials using a modified McMillan-Rowell method.[83,84] Furthermore, all the peaks in $\alpha^2F(\omega)$ for $Ba_{0.625}K_{0.375}BiO_3$ compare well with inelastic-neutron-scattering measurements of the generalized phonon DOS.[26] Even though the quality of their tunneling data deteriorates at high energies, Huang *et al.*[33] have clearly established that high-energy phonons are involved in superconductivity, that the electron-phonon coupling constant $\lambda=1$, and that $2\Delta_0(0)/k_BT_c=3.8\pm0.1$.

Schlesinger and co-workers[22–24] have measured the superconducting energy gap of $Ba_{0.6}K_{0.4}BiO_3$ using infrared spectroscopy. These measurements show an enhancement of the low-frequency reflectivity in the superconducting phase, with a peak in the ratio of the reflectivity in the superconducting state to that in the normal state.[22] An energy-gap ratio of $2\Delta_0(0)/k_BT_c=3.5\pm0.5$ is obtained, consistent with the value from electron-tunneling measurements.

Experiments on the isotope effect,[3,20,42] inelastic neutron scattering,[26–28] infrared reflectivity[22–24] and electron tunneling,[29–35] etc., suggest that $Ba_{1-x}K_xBiO_3$ is a BCS superconductor[85] in which electron-phonon interaction (EPI) plays a significant role.[65,86–89] Therefore, it is timely and of great interest to study theoretically the overall consistency of these experimental results and the nature of superconductivity in this material. The microscopic relation between the EPI and properties of a phonon-mediated superconductor can be described by the Nambu-Eliashberg theory,[90–100] in which the retarded nature of the EPI is properly taken into account. For isotropic superconductors the Eliashberg function $\alpha^2F(\omega)$, which is an EPI weighted phonon density of states, and the Coulomb pseudopotential μ^*, describing the repulsive Coulomb interactions between electrons, are central to the theory.[93] In this paper we construct $\alpha^2F(\omega)$ in a semiempirical manner. The method is primarily based on the phonon density of states calculated from molecular-dynamics simulations. The Coulomb pseudopotential μ^* is determined by fixing T_c from the Eliashberg gap equations to the experimental value T_c^{expt}. Finite-temperature superconducting properties, such as the energy gap Δ_0 and tunneling characteristics, are calculated and compared with available experiments. We attempt to show that a consistent picture of superconductivity in $Ba_{1-x}K_xBiO_3$ can be obtained from the electron-phonon coupling mechanism within Eliashberg theory.

This paper is organized as follows: in Sec. II we present the Eliashberg gap equations at finite temperatures and discuss the kernels. In Sec. III the model for the Eliashberg function $\alpha^2F(\omega)$ based on the MD phonon density of states and tunneling experiments is discussed. Results obtained from the solutions of the Eliashberg gap equations are discussed and compared with available ex-

periments in Sec. IV. In the Sec. V we present some concluding remarks.

II. THEORETICAL BACKGROUND

The electron-phonon interaction is often characterized by the Eliashberg function $\alpha^2F(\omega)$ defined by[93,100]

$$\alpha^2F(\omega)=\sum_{\mathbf{k},\mathbf{k}',\mathbf{q}}|g(\mathbf{k},\mathbf{k}',\mathbf{q})|^2\delta(\varepsilon_{\mathbf{k}}-E_F)\delta(\varepsilon_{\mathbf{k}'}-E_F)\times\delta(\omega-\omega_{\mathbf{q}})/N(0)\ , \tag{1}$$

where $\omega_{\mathbf{q}}$ is the phonon frequency (we use $\hbar=1$), $g(\mathbf{k},\mathbf{k}',\mathbf{q})$ is the screened electron-phonon coupling matrix element, $N(0)$ is the electronic density of states at the Fermi surface, E_F is the electron Fermi energy, and the δ functions restrict the $\mathbf{k}$ and $\mathbf{k}'$ summations to the Fermi surface. This function can be viewed as a product of the phonon density of states $F(\omega)$ and an effective electron-phonon matrix-element square $\alpha^2(\omega)=\alpha^2F(\omega)/F(\omega)$, which represents the strength of the electron-phonon coupling. The dimensionless electron-phonon coupling constant λ is defined by

$$\lambda=2\int_0^\infty\frac{\alpha^2F(\omega)}{\omega}d\omega\ . \tag{2}$$

A. Eliashberg gap equation near T_c

We will start by writing down the Eliashberg gap equations for the energy- and temperature-dependent mass-renormalization function Z and the gap function Δ. Near the transition temperature T_c, these equations can be linearized because the gap approaches zero. The linearized Eliashberg equations for the critical temperature T_c in the imaginary-frequency formalism can be written as[95–99]

$$\Delta(i\omega_n)=\sum_{m=0,\pm1,\ldots}^{|\omega_m|\le\omega_c}\frac{S(n,m)}{|2m+1|}\Delta(i\omega_m)\ , \tag{3}$$

where

$$S(n,m)=\lambda(n-m)-\mu^*(\omega_c)-\delta_{n,m}\sum_{l=0,\pm1,\ldots}^{|\omega_l|\le\omega_c}\lambda(n-l)\mathrm{sgn}(\omega_n)\mathrm{sgn}(\omega_l)\ . \tag{4}$$

In Eqs. (3) and (4), $\Delta(i\omega_n)$ is the energy-dependent gap function and ω_n are the Matsubara frequencies, $\omega_n=\pi k_BT_c(2n+1)$, $n=0,\pm1,\pm2,\ldots$. The frequency summations in Eqs. (3) and (4) are cut off at a maximum value ω_c. The Coulomb pseudopotential μ^* depends upon the cutoff ω_c. The functions $\lambda(n-m)$ is related to $\alpha^2F(\omega)$ through the relation

$$\lambda(n-m)=2\int_0^\infty\frac{\omega\alpha^2F(\omega)d\omega}{\omega^2+(\omega_n-\omega_m)^2}\ . \tag{5}$$

Clearly, $\lambda(0)$ is equal to λ defined in Eq. (2). The numerical method for solving Eq. (3) is discussed by Bergman and Rainer[96] and by Allen and Mitrovic.[99] Using this scheme, the transition temperature T_c can be calculated for a given $\alpha^2F(\omega)$ and μ^*. Alternatively, for a given $\alpha^2F(\omega)$ and T_c^{expt}, one can determine the value of μ^*. Since μ^* changes only slightly as a result of isotopic substitution, using the $\alpha^2F(\omega)$ for the isotopically substituted sample, one can determine the T_c and, therefore, the isotope-effect exponent.

B. Eliashberg gap equations at finite temperature

The Eliashberg gap equations at a temperature T can be written as[93,99]

$$\omega[1-Z(\omega,T)]=\int_0^\infty d\omega'\,\mathrm{Re}\left[\frac{\omega'}{[\omega'^2-\Delta^2(\omega',T)]^{1/2}}\right]\int_0^\infty d\Omega\,\alpha^2F(\Omega)K_+(T,\omega,\omega',\Omega) \tag{6}$$

and

$$\Delta(\omega,T)Z(\omega,T)=\int_0^\infty d\omega'\,\mathrm{Re}\left[\frac{\Delta(\omega',T)}{[\omega'^2-\Delta^2(\omega',T)]^{1/2}}\right]\left[\int_0^\infty d\Omega\,\alpha^2F(\Omega)K_-(T,\omega,\omega',\Omega)-\mu^*\Theta(\omega_c-\omega')\tanh(\tfrac{1}{2}\beta\omega')\right]\ , \tag{7}$$

where $\beta=1/k_BT$. The kernels $K_\pm(T,\omega,\omega',\Omega)$ are defined as

$$K_\pm(T,\omega,\omega',\Omega)=[f(\omega')+n(\Omega)]\left[\frac{1}{\omega+\omega'-\Omega+i0^+}\pm\frac{1}{\omega-\omega'+\Omega+i0^+}\right]+[f(-\omega')+n(\Omega)]\left[\frac{1}{\omega+\omega'+\Omega+i0^+}\pm\frac{1}{\omega-\omega'-\Omega+i0^+}\right]\ , \tag{8}$$

where $f(\omega)$ and $n(\Omega)$ are the Fermi and Bose distributions, respectively. In Eqs. (6) and (7), the functions $\Delta(\omega,T)$ and $Z(\omega,T)$ are the complex temperature- and energy-dependent gap and renormalization functions, respectively. The integrals over $K_\pm$ have both imaginary and principal parts. These nonlinear coupled integral equations can be numerically solved by iterative methods.[101] At a temperature T, the gap edge $\Delta_0(T)$ is defined by the equation

$$\mathrm{Re}[\Delta(\Delta_0(T),T)]=\Delta_0(T)\ . \tag{9}$$

In the weak-coupling BCS limit, $\Delta(\omega,T)$ is taken as a

constant $\Delta(T)$ and the BCS gap equation can be written as[85,102]

$$\ln\left[\frac{\Delta(T)}{\Delta(0)}\right]+2\sum_{m=1}^{\infty}(-1)^{m+1}\kappa_0\left[m\frac{\Delta(T)}{k_BT}\right]=0\ , \qquad (10)$$

where κ_0 is the Hankel function.

III. MODEL OF THE ELIASHBERG FUNCTION $\alpha^2F(\omega)$

We construct a model for $\alpha^2F(\omega)$ using the phonon density of states, $F(\omega)$, and the information from electron-tunneling experiments. Salient features of the calculated phonon density of states and its comparison with neutron and tunneling experiments along with other supporting experimental data used in constructing a model of $\alpha(\omega)$ are discussed below.

A. Phonon density of states $F(\omega)$

Partial and total phonon density of states of $BaBiO_3$ and $Ba_{0.6}K_{0.4}BiO_3$ were calculated using the molecular-dynamics method.[103] Molecular-dynamics simulations were performed in the orthorhombic phase ($a=6.2000$ Å, $b=6.1561$ Å, $c=8.6948$ Å) at the experimental density of 7.88 g/cm^3. Effective interparticle interactions were used in the MD simulations. The potentials[104] include steric repulsion between ions, Coulomb interactions due to charge-transfer effects, and charge-dipole interactions due to the large electronic polarizability of O^{2-} ions. The $Ba_{0.6}K_{0.4}BiO_3$ system was obtained from $BaBiO_3$ by randomly replacing 40% of the Ba atoms with K atoms. The calculations were performed at the experimental density of 7.33 g/cm^3 in the cubic phase (4.3160 Å). Before calculating the phonon DOS, it was ensured that the systems were dynamically stable in the appropriate symmetries at the correct densities. Phonon DOS was calculated using three methods: (1) from the Fourier transform of the velocity autocorrelation function,[104] (2) the equation-of-motion method,[105,106] and (3) direct diagonalization of the dynamical matrix.[81] The results of all these three calculations are in agreement with one another.

The molecular-dynamics partial phonon DOS for $Ba_{0.6}K_{0.4}BiO_3$ is shown in Fig. 2, and the total phonon DOS $F(\omega)$ is shown in Fig. 3(a). There are three significant features in these figures: (1) The DOS below 20 meV is mainly due to Ba, K, and Bi, whereas the region above 20 meV is entirely due to oxygen; (2) the peak at 11 meV in the total DOS is mainly due to Ba and Bi, whereas K and Bi contribute to the peak at 15 meV; and (3) in the DOS beyond 20 meV where the oxygen contribution is dominant, there is a broadband from 25 to 43

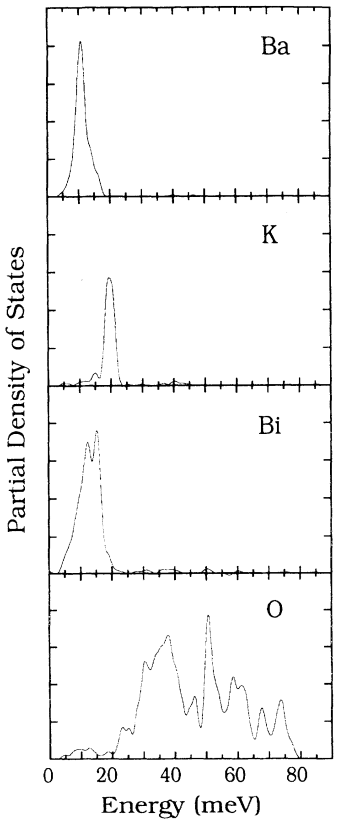

FIG. 2. Partial phonon density of states for Ba, K, Bi, and O in $Ba_{0.6}K_{0.4}BiO_3$ from molecular-dynamics simulations.

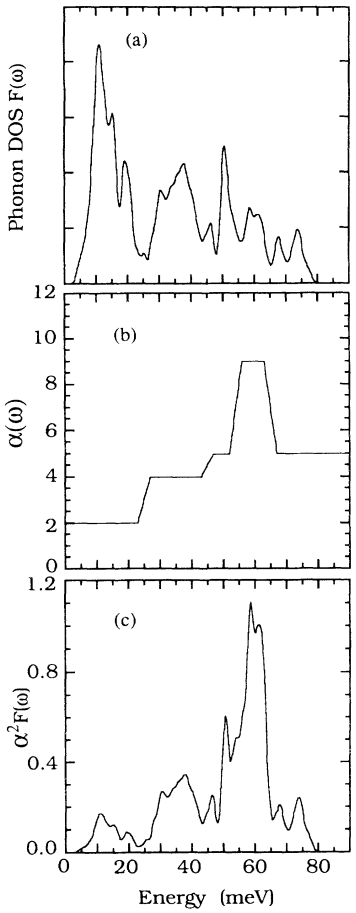

FIG. 3. (a) Total phonon density of states for $Ba_{0.6}K_{0.4}BiO_3$ from molecular-dynamics simulations. (b) Electron-phonon coupling function $\alpha(\omega)$. (c) Eliashberg function $\alpha^2F(\omega)$ for $Ba_{0.6}K_{0.4}BiO_3$.

meV, a peak around 51 meV, a band between 54 and 65 meV, and small peaks at 67 and 73 meV. All of these features have been observed, to within about 10%, in elastic-neutron-scattering measurements[26] of the generalized density of states,[107] $G(\omega)$. In addition, there is a semiquantitative agreement between the positions of the peaks in the MD phonon DOS and the peaks observed in the second derivative of the tunneling current in electron-tunneling experiments.

B. Model for $\alpha(\omega)$

The Eliashberg function is related to $F(\omega)$ through the energy-dependent electron-phonon matrix-element square $\alpha^2(\omega)$ as a weighting factor. In general, different phonon modes may have different contributions to this weighting.[100] However, structures in $F(\omega)$ will be manifested in $\alpha^2F(\omega)$. We divide the phonon energy from 0 to $\omega_{\max}$ (=80 meV) into several segments (bands). This division is chosen such that each band contains either one or several peaks of $F(\omega)$. The detailed manner of this division is not important as long as it is qualitatively consistent with the intensities of peaks in the derivative of the tunneling conductance. We divide the phonon energy into five bands: 0–23, 27–43, 47–52, 56–63, and 67–80 meV. The electron-phonon weighting factor $\alpha(\omega)$ is modeled as a simple function of ω. In the model for $\alpha(\omega)$, these bands are given weights A_1, A_2, A_3, A_4, and A_5, respectively. Linear interpolation is used to connect the region between the bands.

There are several experimental results that restrict the values of $A_1,\ldots,A_5$. First, in electron-tunneling experiments, the dips in the second derivative of the tunneling current with respect to the applied voltage correspond to peaks in the Eliashberg function. The amplitudes of these dips should vary roughly as $\alpha^2F(\omega)/\omega^2$. This allows us to estimate the constants A_i's, apart from an overall scaling factor, in accordance with the relative amplitude of the dips in the second derivative of the tunneling current in the experimental spectrum of Zasadzinski *et al.*[29] The most interesting feature of the tunneling experiment is that there is clear evidence of phonon images at high energies in the range 30–60 meV. Even though the quality of the tunneling data is not adequate for inversion and the accuracy of the experiment is poorer at higher energies, it is clear that the high-energy phonon structure is unambiguously present. This observation, combined with the fact that the intensity in the second derivative of the tunneling current is roughly proportional to $1/\omega^2$ and the low-energy region does not totally overwhelm the second derivative, establishes the fact that strong electron-phonon coupling is present for high-energy phonons. We take the following ratios in our model: $A_1:A_2:A_3:A_4:A_5=1.0:2.0:2.5:4.5:2.5$. The overall scaling factor for these A_i's is determined by fixing the strength of the EPI λ to the experimental value $\lambda=1$ through Eq. (2).

Measurements[47–49] of the upper and lower critical magnetic fields H_{c2} and H_{c1} can give an estimate of the jump in the specific heat through the relation $\Delta C/k_BT_c=(1/8\pi\kappa^2)(dH_{c2}/dT)^2$, where κ is the measured Ginzburg-Landau parameter. This, in conjunction with the BCS relation[85] $\Delta C/k_BT_c=1.43\gamma$ and the expression for the electronic specific-heat coefficient $\gamma=(2\pi^2/3)k_B^2N^*(0)$, gives an upper limit to the EPI renormalized electron density of states $N^*(0)$. If the band-electron density of states, $N(0)$, from band-structure calculations[61] is used, the electron-phonon coupling constant $\lambda=N^*(0)/N(0)-1$ can be estimated. Recent magnetic-field measurements[47] give $\lambda\approx0.9$–1.1. Tunneling experiments[29,33] also give $\lambda\approx1$. Furthermore, the ratio $2\Delta_0(0)/k_BT_c$ is another measure of the degree of the strong electron-phonon coupling. The observed value[22,31,33] of this ratio (3.5–3.8), which is close to the weak-coupling BCS value of 3.52, suggests that λ cannot be too large. Therefore, $\lambda=1$ is a reasonable experimental value.

The function $\alpha(\omega)$ corresponding to $\lambda=1$ is shown in Fig. 3(b). We normalize $F(\omega)$ such that $\int F(\omega)d\omega=1$. Combining this function $\alpha(\omega)$ with $F(\omega)$, we obtain the Eliashberg function $\alpha^2F(\omega)=[\alpha(\omega)]^2F(\omega)$ for the $Ba_{0.6}K_{0.4}BiO_3$ system, which is shown in Fig. 3(c).

C. Moments of $\alpha^2F(\omega)$

The various important properties of $\alpha^2F(\omega)$ are summarized in the Table I, where, following Allen and Dynes,[98] the nth moment of the phonon frequency is defined by

$$\langle\omega_n\rangle=\frac{2}{\lambda}\int_0^\infty\frac{\omega^n\alpha^2F(\omega)d\omega}{\omega}\quad(n=0,1,2,\ldots),\tag{11}$$

and the logarithmic mean phonon frequency is defined by[98]

$$\omega_{\ln}=\lim_{n\to0}\langle\omega_n\rangle^{1/n}=\exp\left[\frac{2}{\lambda}\int_0^\infty\frac{\alpha^2F(\omega)}{\omega}\ln(\omega)d\omega\right].\tag{12}$$

From Table I we note that both the first moment $\langle\omega_1\rangle$ and $\omega_{\ln}$ are quite large (30–40 meV). Roughly speaking,[99] this is the origin of the high critical temperature T_c of this superconductor. The area of the $\alpha^2F(\omega)$ curve is given by $A=\int\alpha^2F(\omega)d\omega=\lambda\langle\omega_1\rangle/2$. This area is also large compared with that of any conventional low-temperature superconductor.[96,98,99] Note that the first moment is slightly larger than $\omega_{\ln}$, since Eq. (12) gives more weight on the low-energy side. However, the total electron-phonon coupling constant is moderate to weak, $\lambda=1$. This is due to large electron-phonon matrix ele-

TABLE I. Moments of $\alpha^2F(\omega)$ for $Ba_{0.6}K_{0.4}BiO_3$.

Moments of $\alpha^2F(\omega)$	
Maximum phonon energy $\omega_{\max}$	80.0 meV
$A=\int_0^\infty\alpha^2F(\omega)d\omega$	19.6 meV
λ	1.0
$\langle\omega_1\rangle$	39.2 meV
$\langle\omega_2\rangle^{1/2}$	44.2 meV
$\omega_{\ln}$	31.1 meV

ments corresponding to the high-energy phonons.

To summarize, in this section we have constructed the Eliashberg function $\alpha^2F(\omega)$ for $Ba_{0.6}K_{0.4}BiO_3$ from the phonon DOS with the help of electron-tunneling data. We have shown that it is possible to have a large electron-phonon matrix element for selected high-energy phonon modes and have $\lambda=1$. We will use our model $\alpha^2F(\omega)$ to study the interdependence of λ, μ^*, and T_c and calculate temperature dependence of the energy gap and tunneling characteristics.

IV. RESULTS AND DISCUSSION

A. Relationship between λ and μ^*

In this section we explore the interrelationship between λ, μ^*, and T_c within the context of our model. Given $\alpha^2F(\omega)$ and $\lambda=1$, we determine μ^* by requiring that the calculated T_c from the linearized Eliashberg equations be equal to the experimental value ($T_c^{\rm expt}=29.5$ K for $x=0.4$). Linearized gap equations, given in Eq. (3), represents a matrix eigenvalue problem and can be solved numerically. We find that the size of the matrix $N_c=100$ [or $\omega_c=\pi k_B T_c(2N_c+1)=1605$ meV] is large enough to give accurate solutions.

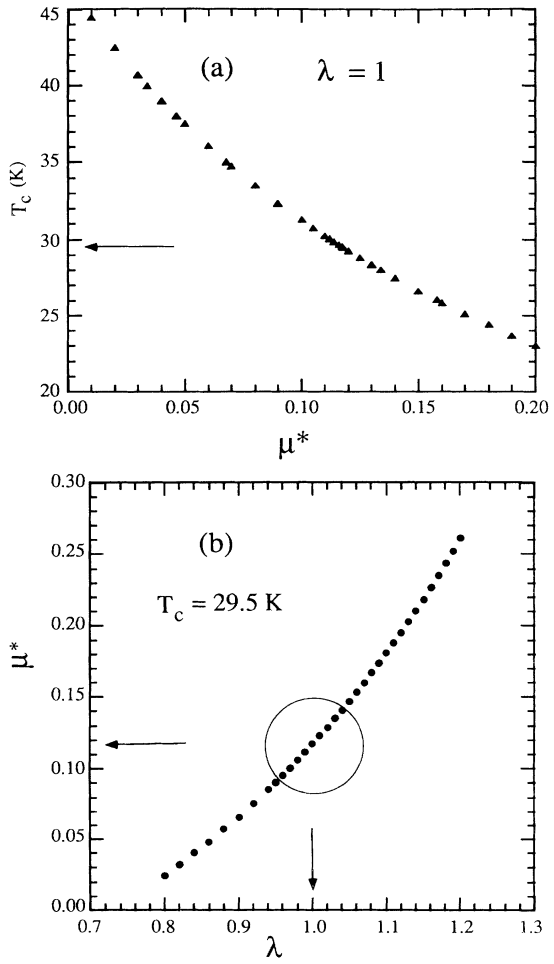

FIG. 4. (a) T_c vs μ^* for a fixed value of $\lambda=1$. The solid triangles are solutions of the Eliashberg gap equations. The arrow indicates the experimental T_c for $Ba_{0.6}K_{0.4}BiO_3$. (b) λ vs μ^* for fixed $T_c=29.5$ K. The values of μ^* for $\lambda=0.93-1.07$ are enclosed in the circle. The arrows indicate the values of μ^* and $\lambda=1$.

For a fixed value of $\lambda=1$, we calculated the values of μ^* for T_c in the range 20–45 K. These results are shown in Fig. 4(a). Clearly, T_c depends strongly on μ^*. In particular, a value of $\mu^*\sim0.10$ can give $T_c\sim31$ K, and $T_c=29.5$ K requires $\mu^*=0.1173$.

The dependence of μ^* on λ for a fixed value of $T_c=29.5$ K is shown in Fig. 4(b). We note that, for λ between 0.95 and 1.10, the corresponding value of μ^* is between 0.09 and 0.16. These values of λ and μ^* are quite reasonable, considering the fact that the experimental estimates of λ is ~1 for $Ba_{1-x}K_xBiO_3$, and $\mu^*=0.1-0.13$ is reasonable for almost all of the known low-temperature superconductors.[99]

Once μ^* is determined from the T_c for the ^{16}O material, the same μ^* can be used to estimate T_c from Eq. (3) for the ^{18}O substitution. Of course, to implement this, one would need an $\alpha^2F(\omega)$ for ^{18}O material. Such a scheme has been implemented[108] to calculate the oxygen (^{16}O,^{18}O) isotope effect in T_c. Using $^{18}\mu^*=^{16}\mu^*=0.1173$, we determine T_c for the ^{18}O system and estimate the oxygen isotope-effect exponent $\alpha_O\approx0.35$. In fact, the value of μ^* changes as a result of isotopic substitution.[93,98] For the fixed frequency cutoff $\omega_c=1605$ meV, it is a simple matter to estimate $^{18}\mu^*=0.1181$ from the value of $^{16}\mu^*=0.1173$, $^{16}\omega_{\rm max}=80$ meV, and $^{18}\omega_{\rm max}=75.4$ meV. When $^{18}\mu^*=0.1181$ is used to calculate $^{18}T_c$ and the oxygen isotope-effect exponent, we obtain $\alpha_O=0.365$. This is in satisfactory agreement with the experimental values of 0.41 ± 0.03 of Hinks *et al.*[42] and 0.35 ± 0.05 of Kondoh *et al.*[20]

B. Solutions of the gap equations at finite temperature

The coupled integral equations (6) and (7) can be solved by the numerical-iteration method.[101] The Coulomb pseudopotential μ^* in both the imaginary- and real-frequency Eliashberg equations depends upon the cutoff ω_c. Since a cutoff at real frequency does not analytically continue to a cutoff at imaginary frequency,[100,109,110] for a given $\alpha^2F(\omega)$, different values of μ^* may needed in order to get a common T_c. We solve Eqs. (6) and (7) using our model $\alpha^2F(\omega)$ and $\omega_c\approx200$ meV. μ^* is determined by fixing the value of the calculated T_c to the experimental value (29.5 K). The value of T_c from Eqs. (6) and (7) is determined by extrapolating the calculated $[\Delta_0(T)]^2$ to zero at high temperatures where $\Delta_0(T)/\Delta_0(0)\sim0.3$. This procedure gives $\mu^*\approx0.15$, which is higher than the value of μ^* used in the imaginary-frequency linearized Eliashberg gap equations with $\omega_c=1605$ meV.

We have solved the coupled integral equations for the complex functions $Z(\omega,T)$ and $\Delta(\omega,T)$ at several temperatures between 0 and T_c. In Figs. 5(a) and 5(b), we give the solutions of the renormalization and gap functions at $T=2$ K. The imaginary parts of the gap $\Delta(\omega,T)$ and the renormalization function $Z(\omega,T)$ are zero below the gap

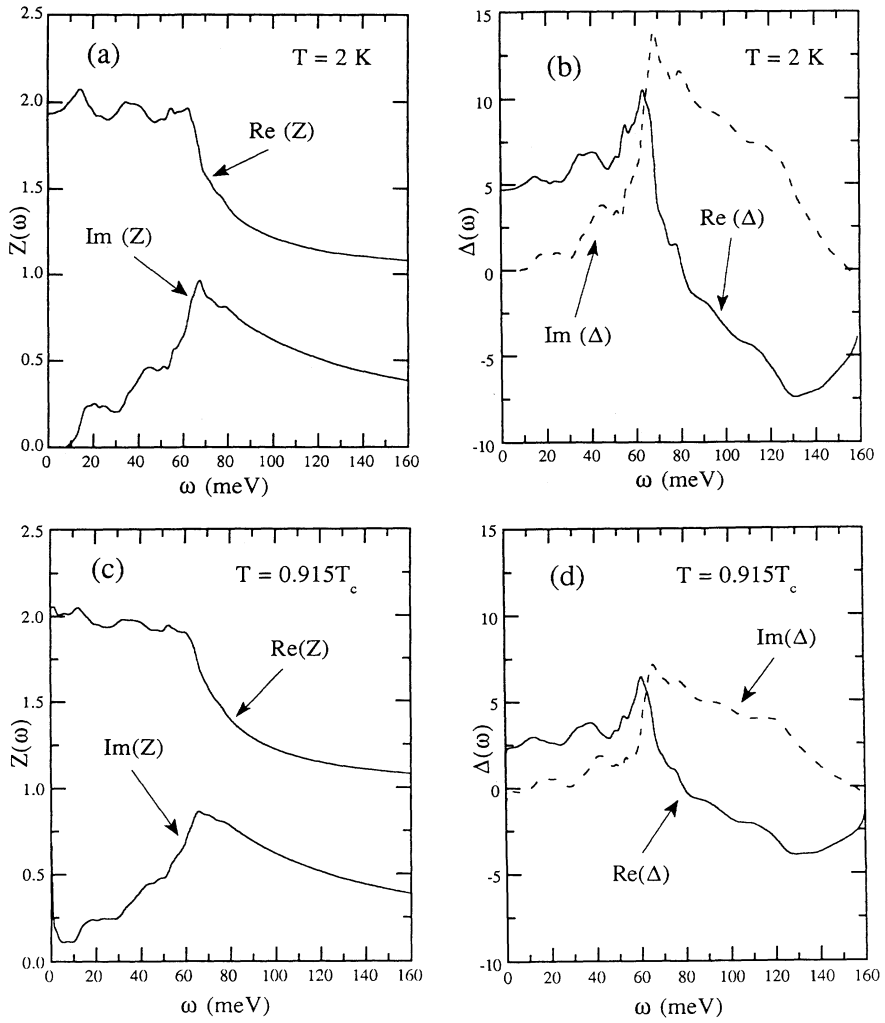

FIG. 5. Real and imaginary parts of energy-dependent renormalization functions $Z(\omega,T)$ and gap functions $\Delta(\omega,T)$ at $T=2$ K and $T=0.915T_c=27$ K.

edge Δ_0. The structure in the Eliashberg function [Fig. 3(c)] and thus the structure in the phonon DOS are reflected in the real and imaginary parts of the gap function $\Delta(\omega,T)$ and renormalization function $Z(\omega,T)$. In Figs. 5(c) and 5(d), we show solutions of $Z(\omega,T)$ and $\Delta(\omega,T)$ at a higher temperature $T=0.915T_c$. The imaginary part of $Z(\omega,T)$ is large and positive, the imaginary part of $\Delta(\omega,T)$ is nonzero and negative for low energies, and as expected, both the real and imaginary parts of $\Delta(\omega,T)$ at $T=0.915T_c$ are reduced from their low-temperature values.

The gap edge can be calculated using Eq. (9). At zero temperature, $\Delta_0(0)=4.749$ meV, and at $T=0.915T_c=27$ K, the gap edge is $\Delta_0(T)=2.353$ meV. The temperature variation of the reduced gap, $\Delta_0(T)/\Delta_0(0)$, is shown in Fig. 6. The deviation of the reduced gap from the BCS value is small, and the size of this deviation is consistent with $\lambda=1$. The ratio $2\Delta_0(0)/k_BT_c$ calculated from the Eliashberg equations is 3.75 ± 0.1, in agreement with the values 3.5 ± 0.5 and 3.8 ± 0.1 obtained from the infrared[22] and tunneling[31,33] experiments.

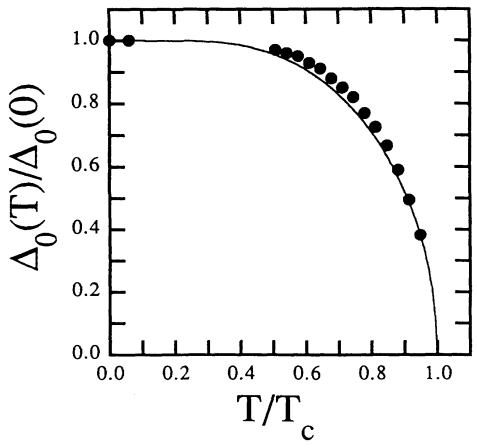

FIG. 6. Reduced gap $\Delta_0(T)/\Delta_0(0)$ calculated from Eliashberg gap equations as a function of the reduced temperature T/T_c. The solid curve is calculated from the BCS gap equation [Eq. (10)].

C. Electron tunneling

Once $\Delta(\omega,T)$ and $Z(\omega,T)$ are known, many superconducting properties can be easily calculated.[93,94] The tunneling current in a superconductor–insulator–normal-metal junction at finite T can be computed from[92–94]

$$I(V)\propto\int_{-\infty}^{\infty}d\omega\,\tilde{\rho}(\omega,T)[f(\omega)-f(\omega+V)]\ , \tag{13}$$

where V is the applied voltage and $\rho(\omega,T)$ is the normalized quasiparticle tunneling density of states, which is related to the complex gap function $\Delta(\omega,T)$ through[92–94]

$$\tilde{\rho}(\omega,T)=\mathrm{Re}\left[\frac{\omega}{[\omega^2-\Delta^2(\omega,T)]^{1/2}}\right]\ . \tag{14}$$

In Figs. 7(a) and 7(b) we show the calculated tunneling second derivative $d\sigma(V)/dV$ at $T=2$ and 27 K, respectively, where $\sigma(V)$ is the tunneling conductance, normalized to the tunneling conductance in the normal state ($\Delta=0$) at the same temperature:

$$\sigma(V)=\left[\frac{dI}{dV}\right]_s\Big/\left[\frac{dI}{dV}\right]_n\ . \tag{15}$$

Strong features in the energy range 30–60 meV can be seen in Fig. 7(a). As we expected, the overall features in the calculated results are similar to the experimental tunneling spectra,[29] which are also measured near 2–5 K. However, the amplitude of the calculated results around 60 meV is considerably larger than in the experimental spectra. This is due, in part, to experimental difficulties in observing structures at high voltages.[33] It is also possible that the relative weight given to the frequency band around 60 meV in our model is larger than needed. Reducing the weight around 60 meV in our model of $\alpha(\omega)$, keeping $\lambda=1$ fixed, has the effect of increasing relative weights of other parts of the spectrum in $\alpha^2F(\omega)$. Such a modified model does not change the results in any significant manner. All the conclusions discussed in this paper remain unchanged. Resolution of this issue requires tunneling experiments with better resolution at higher energies. The calculated tunneling second derivative at $T=0.915T_c$ is shown in Fig. 7(b). We note that thermal effects smear out the strong dip structures seen at low temperatures.

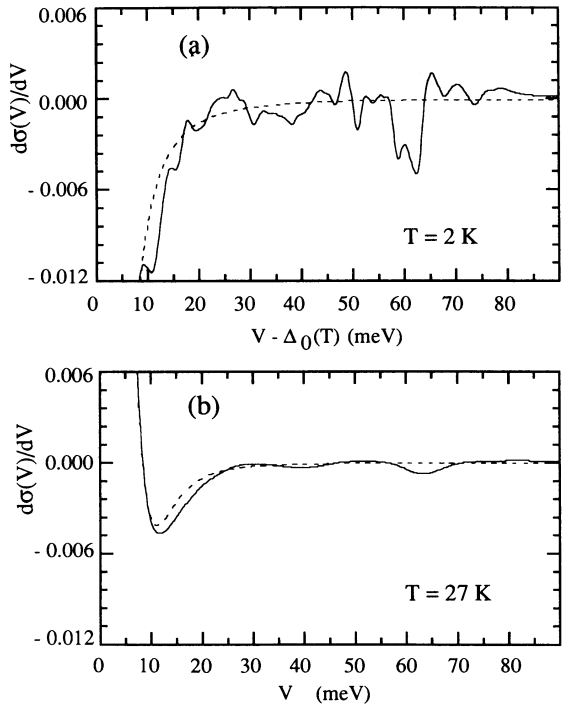

FIG. 7. Calculated tunneling second derivatives at (a) $T=2$ K and (b) $T=0.915T_c=27$ K. The dashed curves are the BCS results.

V. CONCLUDING REMARKS

In this section we would like to remark on three interrelated topics: (1) how reliable are the various formulas for calculating T_c of this material; (2) what T_c is in the strong-coupling limit $\lambda=2-3$, given the fact that the proposed model [$\alpha^2F(\omega)$ with $\lambda=1$ and $\mu^*=0.1173$] provides a reasonable description of the superconducting properties of $Ba_{1-x}K_xBiO_3$; and (3) difficulties in obtaining $\alpha^2F(\omega)$ at higher energies from the inversion of the tunneling data.

To address (1) and (2), we have calculated T_c as a function of λ for a fixed value of $\mu^*=0.1173$. Nothing is changed except the value of λ by scaling the function $\alpha^2F(\omega)$. Linearized Eliashberg gap equations are solved to determine T_c. Results are shown in Fig. 8. For com-

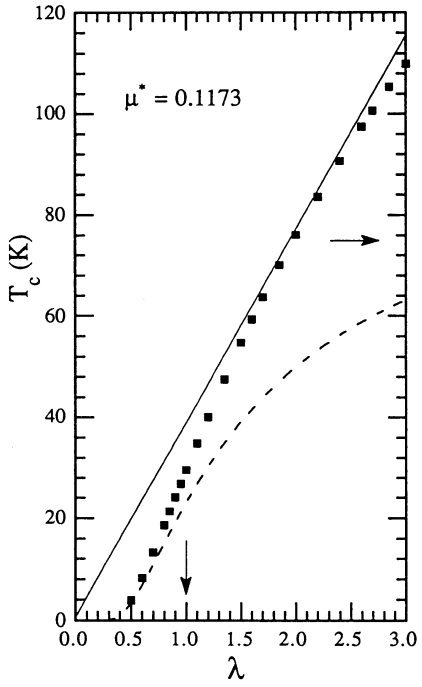

FIG. 8. T_c as a function of λ for a fixed value of $\mu^*=0.1173$. The solid squares are from the solution of the Eliashberg gap equations. The dashed curve is based on the McMillan-Allen-Dynes equation [Eq. (16)]. The arrow at $\lambda=1$ corresponds to $T_c=29.5$ K from Eliashberg gap equations and 23.05 K from Eq. (16). For $\lambda=3$ and $\mu^*=0.1173$, Eq. (16) gives $T_c=63.11$ K and, with $\lambda=3$ and $\mu^*=0$, a value of $T_c=75.16$ K (indicated by an arrow). The solid line is based on Eq. (17).

parison, we also show in Fig. 8 the approximate results obtained from the McMillan-Allen-Dynes[95,98] formula for T_c,

$$T_c=\frac{\omega_{\ln}}{1.20}\exp\left[-\frac{1.04(1+\lambda)}{\lambda-\mu^*(1+0.62\lambda)}\right], \quad (16)$$

where $\omega_{\ln}$ is defined in Eq. (12), and listed in the Table I. In Fig. 8, for $\lambda\geq 2$, there are large deviations between the exact solutions and the values of T_c from Eq. (16). In general, Eq. (16) underestimates T_c. For example, $T_c\approx 23$ K from Eq. (16) with $\lambda=1.0$ and $\mu^*=0.1173$, which is close but lower than the exact value (29.5 K) from the gap equations. A better estimate of T_c can be obtained from a more complicated formula given by Allen and Dynes[98] [see Eqs. (34)–(38) of Ref. 98], which, for $\lambda=3$ and $\mu^*=0.1173$, gives a value of $T_c=86.5$ K.

The point of the above calculation is to demonstrate from the solution of the Eliashberg gap equations that when there is substantial coupling of the carriers to the high-energy phonons, there is no inherent problem in having a $T_c\approx 100$ K in the strong-coupling limit $\lambda=3$. Approximate formulas to estimate T_c lead to the opposite conclusion. We wish to emphasize that no claim is made whether a material with $\lambda=3$ exists or that layered cuprates are the strong-coupling limit of this material.

We have investigated the issue of maximum T_c using the scheme proposed by Leavens.[111,112] In this scheme the maximum T_c is a given by[100,111]

$$T_c^{\max}(\lambda)=C(\mu^*)A(\lambda), \quad (17)$$

where C is a universal function of μ^* and A is the area under $\alpha^2F(\omega)$. For the value of $\mu^*=0.1173$ used in our imaginary-frequency calculations, $C(\mu^*=0.1173)=0.17$ can be read from Fig. 2 of Leavens.[111] Using our value of $A(\lambda=1)=19.6$ meV from Table I and the condition that the shape of $\alpha^2F(\omega)$ remain fixed as λ is increased, we can write the expression for $T_c^{\max}$ (K) $=0.17\times 11.6\times 19.6\lambda=38.6\lambda$. It is indeed quite interesting that this formula provides such a good estimate of maximum T_c for large values of λ (see Fig. 8).

For the $Ba_{1-x}K_xBiO_3$ system, earlier attempts to invert the tunneling data of Zasadzinski *et al.* were not successful.[29] This is mainly due to two experimental uncertainties. The value of $\alpha^2F(\omega)$ at high energies are important for $Ba_{1-x}K_xBiO_3$. However, large background-noise conductance at high voltage makes experimental observation of structures at high voltage difficult.[29,33,60] Therefore, accurate tunneling spectra for energies ≥ 60 meV are not easy to obtain. In addition, the low-energy (≤ 15 meV) parts of the Eliashberg function are usually difficult to extract from tunneling data with polycrystalline samples.[31] Recently, Huang *et al.*[33] have been able to invert their point-contact tunneling data to obtain $\alpha^2F(\omega)$ for $Ba_{0.625}K_{0.375}BiO_3$. The overall shape of their inverted $\alpha^2F(\omega)$ is in qualitative agreement with our model. It is clear, however, that, because of difficulties in obtaining tunneling data at higher voltage, the $\alpha^2F(\omega)$ obtained by inversion is missing some contribution at higher energies.

To summarize, we have studied the nature of superconductivity in cubic $Ba_{1-x}K_xBiO_3$. We have constructed a model of the electron-phonon Eliashberg function for $Ba_{0.6}K_{0.4}BiO_3$. Superconducting properties calculated using the Eliashberg equations are consistent with experiments. We conclude that coupling of electrons to high-energy oxygen phonons provides a reasonable description of superconductivity in this material within the framework of Eliashberg theory.

ACKNOWLEDGMENTS

We would like to thank Dr. Chun-Keung Loong and Qiang Huang for valuable discussions. We also thank Dr. A. Nakano for a critical reading of this manuscript. W.J. would like to acknowledge the support, during his stay at the Argonne National Laboratory, from the National Science Foundation (DMR 88-09854) through the Science and Technology Center for Superconductivity. M.H.D. would like to thank Fundacão de Amparo a Pesquisa do Estado de São Paulo (FAPESP), Brazil for support. This work was supported in part by a grant from Louisiana Education Quality Support Fund [No. LEQSF-(1991-92)-RD-A-05].

*Permanent address: Instituto de Física e Química de São Carlos–USP, São Carlos, Brazil.

[1]L. F. Mattheiss, E. M. Gyorgy, and D. W. Johnson, Jr., Phys. Rev. B **37**, 3745 (1988).

[2]R. J. Cava, B. Batlogg, J. J. Krajewski, R. Farrow, L. W. Rupp, Jr., A. E. White, K. Short, W. F. Peck, and T. Kometani, Nature **332**, 814 (1988).

[3]B. Batlogg, R. J. Cava, L. W. Rupp, Jr., A. M. Mujsce, J. J. Krajewski, J. P. Remeika, W. F. Peck, Jr., A. S. Cooper, and G. P. Espinosa, Phys. Rev. Lett. **61**, 1670 (1988).

[4]L. F. Schneemeyer, J. K. Thomas, T. Siegrist, B. Batlogg, L. W. Rupp, R. L. Opila, R. J. Cava, and D. W. Murphy, Nature **335**, 421 (1988).

[5]R. J. Cava and B. Batlogg, MRS Bull. **14** (1), 49 (1989).

[6]B. Batlogg, in *Mechanisms of High Temperature Superconductivity,* edited by H. Kamimura and A. Oshiyama (Springer-Verlag, Berlin, 1989), p. 324.

[7]B. Batlogg, R. J. Cava, L. F. Schneemeyer, and G. P. Espinosa, IBM J. Res. Dev. **33**, 208 (1989).

[8]D. G. Hinks, B. Dabrowski, J. D. Jorgensen, A. W. Mitchell, D. R. Richards, S. Pei, and D. Shi, Nature **333**, 836 (1988).

[9]D. G. Hinks, D. R. Richards, B. Dabrowski, A. W. Mitchell, J. D. Jorgensen, and D. T. Marx, Physica C **156**, 477 (1988).

[10]D. G. Hinks, A. W. Mitchell, Y. Zheng, D. R. Richards, and B. Dabrowski, Appl. Phys. Lett. **54**, 1585 (1989).

[11]N. L. Jones, J. B. Parise, R. B. Flippen, and A. W. Sleight, J. Solid State Chem. **78**, 319 (1989).

[12]S. Jin, T. H. Tiefel, R. C. Sherwood, A. P. Ramirez, E. M. Gyorgy, G. W. Kammlott, and R. A. Fastnacht, Appl. Phys. Lett. **53**, 1116 (1988).

[13]S. Kondoh, M. Sera, K. Fukuda, Y. Ando, and S. Sato, Solid State Commun. **67**, 879 (1988).

[14]T. J. Folkerts, R. N. Shelton, and H. B. Radousky, Physica C **162-164**, 550 (1989).

[15]J. C. Phillips, *Physics of High-T_c Superconductors* (Academic, San Diego, 1989).

[16]*High Temperature Superconductivity—The Los Alamos Symposium,* edited by K. S. Bedell, D. Coffey, D. E. Meltzer, D. Pines, and J. R. Schrieffer (Addison-Wesley, Redwood, CA, 1990).

[17]S. Pei, J. D. Jorgensen, D. G. Hinks, B. Dabrowski, D. R. Richards, A. W. Mitchell, Y. Zheng, J. M. Newsam, S. K. Sinha, D. Vaknin, and A. J. Jacobson, Physica C **162-164**, 556 (1989).

[18]S. Pei, J. D. Jorgensen, D. G. Hinks, B. Dabrowski, D. R. Richards, A. W. Mitchell, S. K. Sinha, D. Vaknin, J. M. Newsam, and A. J. Jacobson, in *Oxygen Disorder Effects in High-T_c Superconductors,* edited by I. L. Moran-Lopez and I. K. Schuller (Plenum, New York, 1990), p. 1.

[19]S. Pei, J. D. Jorgensen, B. Dabrowski, D. G. Hinks, D. R. Richards, A. W. Mitchell, J. M. Newsam, S. K. Sinha, D. Vaknin, and A. J. Jacobson, Phys. Rev. B **41**, 4126 (1990).

[20]S. Kondoh, M. Sera, Y. Ando, and M. Sato, Physica C **157**, 469 (1989).

[21]Y. J. Uemura, B. J. Sternlieb, D. E. Cox, J. H. Brewer, R. Kadono, J. R. Kempton, R. F. Kiefl, S. R. Kreitzman, G. M. Luke, P. Mulhern, T. Riseman, D. L. Williams, W. J. Kossler, X. H. Yu, C. E. Stronach, M. A. Subramanian, J. Gopalakrishnan, and A. W. Sleight, Nature **335**, 151 (1988).

[22]Z. Schlesinger, R. T. Collins, J. A. Calise, D. G. Hinks, A. W. Mitchell, Y. Zheng, B. Dabrowski, N. E. Bickers, and D. J. Scalapino, Phys. Rev. B **40**, 6862 (1989).

[23]R. T. Collins, Z. Schlesinger, F. Holtzberg, C. Feild, G. Koren, A. Gupta, D. G. Hinks, A. W. Mitchell, Y. Zheng, and B. Dabrowski, in *Strong Correlation and Superconductivity,* edited by H. Fukuyama, S. Maekawa, and A. P. Malozemoff (Springer-Verlag, Berlin, 1989), p. 289.

[24]Z. Schlesinger and R. T. Collins, MRS Bull. **15** (6), 38 (1990).

[25]K. F. McCarty, H. B. Radousky, D. G. Hinks, Y. Zheng, A. W. Mitchell, T. J. Folkerts, and R. N. Shelton, Phys. Rev. B **40**, 2662 (1989).

[26]C. K. Loong, P. Vashishta, R. K. Kalia, M. H. Degani, D. L. Price, J. D. Jorgensen, D. G. Hinks, B. Dabrowski, A. W. Mitchell, D. R. Richards, and Y. Zheng, Phys. Rev. Lett. **62**, 2628 (1989).

[27]C. K. Loong, D. G. Hinks, P. Vashishta, W. Jin, R. K. Kalia, M. H. Degani, D. L. Price, J. D. Jorgensen, B. Dabrowski, A. W. Mitchell, D. R. Richards, and Y. Zheng, Phys. Rev. Lett. **66**, 3217 (1991).

[28]C. K. Loong, D. G. Hinks, W. Jin, M. H. Degani, D. L. Price, J. D. Jorgensen, B. Dabrowski, A. W. Mitchell, D. R. Richards, Y. Zheng, P. Vashishta, and R. K. Kalia, in *Electron-Phonon Interaction in Oxide Superconductors,* edited by J. P. Carbotte and R. Baquero (World Scientific, Singapore, in press).

[29]J. F. Zasadzinski, N. Tralshawala, D. G. Hinks, B. Dabrowski, A. W. Mitchell, and D. R. Richards, Physics C **158**, 519 (1989).

[30]J. F. Zasadzinski, N. Tralshawala, J. Timpf, D. G. Hinks, B. Dabrowski, A. W. Mitchell, and D. R. Richards, Physics C **162-164**, 1053 (1989).

[31]H. Sato, H. Takagi, and S. Uchida, Physica C **169**, 391 (1990).

[32]F. Morales, R. Escudero, D. G. Hinks, and Y. Zheng, Physics C **169**, 294 (1990); Physica B **169**, 705 (1991).

[33]Q. Huang, J. F. Zasadzinski, N. Tralshawala, K. E. Gray, D. G. Hinks, J. L. Peng, and R. L. Greene, Nature **347**, 369 (1990).

[34]Q. Huang, J. F. Zasadzinski, K. E. Gray, D. R. Richards, and D. G. Hinks, Appl. Phys. Lett. **57**, 2356 (1990).

[35]J. F. Zasadzinski, N. Tralshawala, Q. Huang, K. E. Gray, and D. G. Hinks, IEEE Trans. Magn. **MAG-27**, 833 (1991).

[36]F. Sharifi *et al.*, Bull. Am. Phys. Soc. **36**, 526 (1991); F. Sharifi, A. Pargellis, and R. C. Dynes, Phys. Rev. Lett. **67**, 509 (1991).

[37]S. Pei, N. J. Zaluzec, J. D. Jorgensen, B. Dabrowski, D. G. Hinks, A. W. Mitchell, and D. R. Richards, Phys. Rev. B **39**, 811 (1989).

[38]T. J. Wagener, H. M. Meyer III, D. M. Hill, Y. Hu, M. B. Jost, J. H. Weaver, D. G. Hinks, B. Dabrowski, and D. R. Richards, Phys. Rev. B **40**, 4532 (1989).

[39]Y. Jeon, G. Liang, J. Chen, M. Croft, M. W. Ruckman, D. Di Marzio, and M. S. Hegde, Phys. Rev. B **41**, 4066 (1990).

[40]H. Sato, S. Tajima, H. Takagi, and S. Uchida, Nature **338**, 241 (1989).

[41]M. Sato, S. Kondoh, and M. Sera, in *Strong Correlation and Superconductivity,* edited by H. Fukuyama, S. Maekawa, and A. P. Malozemoff (Springer-Verlag, Berlin, 1989), p. 341.

[42]D. G. Hinks, D. R. Richards, B. Dabrowski, D. T. Marx, and A. W. Mitchell, Nature **335**, 419 (1988).

[43]S. E. Stupp, M. E. Reeves, D. M. Ginsberg, D. G. Hinks, B. Dabrowski, and K. G. Vandervoort, Phys. Rev. B **40**, 10 878 (1989).

[44]M. F. Hundley, J. D. Thompson, and G. H. Kwei, Solid State Commun. **70**, 1155 (1989).

[45]G. H. Kwei, J. A. Goldstone, A. C. Lawson, Jr., J. D. Thompson, and A. Williams, Phys. Rev. B **39**, 7873 (1989).

[46]J. E. Graebner, L. F. Schneemeyer, and J. K. Thomas, Phys. Rev. B **39**, 9682 (1989).

[47]W. K. Kwok, U. Welp, G. W. Grabtree, K. G. Vandervoot, R. Hulscher, Y. Zheng, B. Dabrowski, and D. G. Hinks, Phys. Rev. B **40**, 9400 (1989).

[48]U. Welp, W. K. Kwok, G. W. Crabtree, H. Claus, K. G. Vandervoort, B. Dabrowski, A. W. Mitchell, D. R. Richards, D. T. Marx, and D. G. Hinks, Physics C **156**, 27 (1988).

[49]G. W. Crabtree, W. K. Kwok, U. Welp, K. G. Vandervoort, B. Dabrowski, and D. G. Hinks, Physica B **163**, 652 (1990).

[50]S. D. Peacor, R. A. Richardson, J. Burm, C. Uher, and A. B. Kaiser, Phys. Rev. B **42**, 2684 (1990); C. Uher, J. Superconduct. **3**, 337 (1990).

[51]M. Sera, S. Kondoh, and M. Sato, Solid State Commun. **68**, 647 (1988).

[52]J. P. Wignacourt, J. S. Swinnea, H. Steinfink, and J. B. Goodenough, Appl. Phys. Lett. **53**, 1753 (1988).

[53]S. M. Heald, D. DiMarizo, M. Croft, M. S. Hegde, S. Li, and M. Greenblatt, Phys. Rev. B **40**, 8828 (1989).

[54]M. S. Hegde, P. Barboux, C. C. Chang, J. M. Tarascon, T. Venkatesan, X. D. Wu, and A. Inam, Phys. Rev. B **39**, 4752 (1989).

[55]E. A. Hewat, C. Chaillout, M. Godinho, M. F. Gorius, and M. Marezio, Physica C **157**, 228 (1989).

[56]J. E. Schirber, B. Morosin, and D. S. Ginley, Physica C **157**, 237 (1989).

[57]S. Sugai, Y. Enomoto, and T. Murakami, Solid State Commun. **72**, 1193 (1989).

[58]R. C. Taylor, M. M. Plechaty, D. B. Beach, J. F. Bringley, and M. W. Shafer, Physica C **169**, 35 (1990).

[59]N. V. Anshukova, V. B. Ginodman, A. I. Golovashkin, L. N. Zherikhina, L. I. Ivanova, A. P. Rusakov, and A. M. Tskhovrebov, Zh. Eksp. Teor. Fiz. **97**, 1635 (1990) [Sov. Phys.—JETP **70**, 923 (1990)].

[60]A. N. Pargellis, F. Sharifi, B. Miller, E. S. Hellman, J. M. Rosamilia, and E. H. Hartford, Jr., Appl. Phys. Lett. **58**, 95 (1991).

[61]L. M. Mattheiss and D. R. Hamann, Phys. Rev. Lett. **60**, 2681 (1988).
[62]T. M. Rice, Nature **332**, 780 (1988); P. Prelovsek, T. M. Rice, F. C. Zhang, and A. Klostermann, Physica B **148**, 268 (1987).
[63]N. d'Ambrumenil, Nature, **335**, 113 (1988); P. B. Allen, *ibid.* **335**, 396 (1988).
[64]C. M. Varma, Phys. Rev. Lett. **61**, 2713 (1988); in *High Temperature Superconductors,* edited by T. Akachi, J. A. Cogordan, A. A. Valladares (World Scientific, Singapore, 1989), p. 35.
[65]P. B. Allen, Nature **339**, 428 (1989).
[66]M. D. Nuñez Regueiro and A. A. Aligia, Phys. Rev. Lett. **61**, 1889 (1988); A. A. Aligia, M. D. Nuñez Regueiro, and E. R. Gagliano, Phys. Rev. B **40**, 4405 (1989); A. A. Aligia and M. Baliña, in *Condensed Matter Theories,* edited by A. N. Proto and J. Aliaga (Plenum, New York, in press), Vol. 7.
[67]K. Machida, Physica C **156**, 276 (1988); in *Studies of High Temperature Superconductors,* edited by A. V. Narlikar (Nova Science, New York, 1989), Vol. 1, Chap. 2.
[68]M. J. Rice and Y. R. Wang, Physica C **157**, 192 (1989); J. Yu, X. Y. Chen, and W. P. Su, Phys. Rev. B **41**, 344 (1990).
[69]A. M. Bratkovsky and S. N. Rashkeev, Phys. Lett. A **142**, 172 (1989).
[70]H. C. Gupta, Physica C **158**, 153 (1989).
[71]R. Micnas, J. Ranninger, and S. Robaszkiewicz, Rev. Mod. Phys. **62**, 113 (1990).
[72]D. N. Manh, D. Mayou, and F. Cyrot-Lackmann, Europhys. Lett. **13**, 167 (1990); Solid State Commun. **79**, 723 (1991).
[73]D. A. Papaconstantopoulos, G. D. Drew, F. Cyrot-Lackmann, A. Pasturel, and J. P. Julien, Physica C **162-164**, 1435 (1989); D. A. Papaconstantopoulos, A. Pasturel, J. P. Julien, and F. Cyrot-Lackmann, Phys. Rev. B **40**, 8844 (1989).
[74]M. Shirai, N. Suzuki, and K. Motizuki, J. Phys. Condens. Matter **1**, 2939 (1989); **2**, 3553 (1990); Solid State Commun. **73**, 633 (1990); in *Phonons 89,* edited by S. Hunklinger, W. Ludwig, and G. Weiss (World Scientific, Singapore, 1990), p. 268.
[75]O. Navarro and R. Escudero, Physica C **170**, 405 (1990).
[76]P. Blaha, K. Schwarz, G. Vielsack, and W. Weber, in *Electronic Properties of High-T_c Superconductors and Related Compounds,* edited by H. Kuzmany, M. Mchring, and J. Fink (Springer-Verlag, Berlin, Heidelberg, 1990), p. 343.
[77]Z. Huang and R. E. Allen, Physica C **173**, 173 (1991).
[78]A. Bansil and S. Kaprzyk, Phys. Rev. B **43**, 10335 (1991).
[79]S. Hoen, W. N. Creager, L. C. Bourne, M. F. Crommie, T. W. Barbee III, M. L. Cohen, A. Zettl, L. Bernardez, and J. Kinney, Phys. Rev. B **39**, 2269 (1989); M. K. Crawford, W. E. Farneth, E. M. McCarron III, R. L. Harlow, and A. H. Moudden, Science **250**, 1390 (1990); M. K. Crawford, M. N. Kunchur, W. E. Farneth, E. M. McCarron III, and S. J. Poon, Phys. Rev. B **41**, 282 (1990); J. P. Franck, J. Jung, M. A. K. Mohamed, S. Gygax, and I. G. Sproule, Physica B **169**, 697 (1991).
[80]P. Vashishta, M. H. Degani, and R. K. Kalia, in *Correlations in Electronic and Atomic Fluids,* edited by P. Jena, R. K. Kalia, P. Vashishta, and M. P. Tosi (World Scientific, Singapore, 1990), p. 223.
[81]M. H. Degani, R. K. Kalia, and P. Vashishta, in *Strongly Coupled Plasma Physics,* edited by S. Ichirmaru (Elsevier, New York, 1990), p. 385; in *Condensed Matter Theories,* edited by V. C Aguilera-Navarro (Plenum, New York, 1990), Vol. 5, p. 151.
[82]M. H. Degani, P. Vashishta, and P. K. Kalia, Bull. Am. Phys. Soc. **35**, 204 (1990).
[83]W. L. McMillan and J. M. Rowell, Phys. Rev. Lett. **14**, 108 (1965); in *Superconductivity,* edited by R. D. Parks (Dekker, New York, 1969), Vol. 1, Chap. 11, p. 561.
[84]E. L. Wolf and G. B. Arnold, Phys. Rep. **91**, 31 (1982).
[85]J. R. Schrieffer, *Theory of Superconductivity* (Benjamin, New York, 1964).
[86]D. G. Hinks, B. Dabrowski, D. R. Richards, J. D. Jorgensen, S. Pei, and J. F. Zasadzinski, Physics C **162-164**, 1405 (1989).
[87]D. G. Hinks, in *High Temperature Superconductors,* edited by T. Akachi, J. A. Cogordan, and A. A. Valladares (World Scientific, Singapore, 1989), p. 69.
[88]D. G. Hinks, B. Dabrowski, D. R. Richards, J. D. Jorgensen, S. Pei, and J. F. Zasadzinski, in *High-Temperature Superconductors: Relationship between Properties, Structure, and Solid State Chemistry,* edited by J. D. Jorgensen, K. Kitazaur, J. M. Tarascon, M. S. Thompson, and J. B. Torrance, MRS Symposia Proceedings No. 156 (Materials Research Society, Pittsburgh, 1989), p. 357.
[89]D. G. Hinks, MRS Bulletin **15**, No. 6, 55 (1990).
[90]Y. Nambu, Phys. Rev. **117**, 648 (1960); P. Morel and P. W. Anderson, *ibid.* **125**, 1263 (1962).
[91]G. M. Eliashberg, Zh. Eksp. Teor. Fiz. **38**, 966 (1960) [Sov. Phys.—JETP **11**, 696 (1960)]; **39**, 1437 (1961) [**12**, 1000 (1961)].
[92]D. J. Scalapino, J. R. Schrieffer, and J. W. Wilkins, Phys. Rev. **148**, 263 (1966); D. J. Scalapino, Y. Wada, and J. C. Swihart, Phys. Rev. Lett. **14**, 102 (1965).
[93]D. J. Scalapino, in Superconductivity, edited by R. D. Parks (Dekker, New York, 1969), Vol. 1, p. 449.
[94]V. Ambegaokar, in *Many-Body Physics,* edited by C. DeWitt and R. Balian (Gordon and Breach, New York, 1968), p. 297.
[95]W. L. McMillan, Phys. Rev. **167**, 331 (1968).
[96]G. Bergmann and D. Rainer, Z. Phys. **263**, 59 (1973).
[97]D. Rainer, in *Progress in Low Temperature Physics,* edited by D. F. Brewer (North-Holland, Amsterdam, 1986), Vol. 10, p. 371.
[98]P. B. Allen and R. C. Dynes, Phys. Rev. B **12**, 905 (1975); J. Phys. C **8**, L158 (1975).
[99]P. B. Allen and B. Mitrovic, in *Solid State Physics,* edited by H. Ehrenreich, F. Seitz, and D. Turnbull (Academic, New York, 1982), Vol. 37, p. 1.
[100]J. P. Carbotte, Rev. Mod. Phys. **62**, 1027 (1990).
[101]P. Vashishta and J. P. Carbotte, J. Low Temp. Phys. **10**, 551 (1973); **18**, 457 (1975); J. P. Carbotte, in *Low Temperature Physics-LT13,* edited by K. D. Timmerhaus, W. J. O'Sullivan, and E. F. Hammel (Plenum, New York, 1974), Vol. 3, p. 587.
[102]I. M. Khalatnikov and A. A. Abrikosov, Adv. Phys. **8**, 45 (1959).
[103]A. Rahman and P. Vashishta, in *Physics of Superionic Conductors,* edited by J. W. Perram (Plenum, New York, 1983), p. 93.
[104]P. Vashishta and A. Rahman, Phys. Rev. Lett. **40**, 1337 (1978); P. Vashishta, R. K. Kalia, and I. Ebbsjö, Phys. Rev. B **39**, 6034 (1989).
[105]M. F. Thorpe and R. Alben, J. Phys. C **9**, 2555 (1976).
[106]D. Beeman and R. Alben, Adv. Phys. **26**, 339 (1977).
[107]D. L. Price and K. Sköld, in *Neutron Scattering,* edited by K. Sköld and D. L. Price (Academic, Orlando, 1986), Chap. 1, p. 29.
[108]W. Jin, C. K. Loong, R. K. Kalia, and P. Vashishta, Bull. Am. Phys. Soc. **36**, 525 (1991); W. Jin, C. K. Loong, D. G. Hinks, P. Vashishta, R. K. Kalia, M. H. Degani, D. L. Price, J. D. Jorgensen, and B. Dabrowski, in *Defects in Materials,* edited by P. D. Bristowe, J. E. Epperson, J. E. Griffith, and Z.

L. Weber, MRS Symposia Proceedings No. 209 (Materials Research Society, Pittsburgh, 1991), p. 895.
[109]H. J. Vidberg and J. W. Serene, J. Low Temp. Phys. **29**, 179 (1977).
[110]C. R. Leavens and E. W. Fenton, Solid State Commun. **33**, 597 (1980).
[111]C. R. Leavens, Solid State Commun. **17**, 1499 (1975).
[112]C. R. Leavens, J. Phys. F **7**, 1911 (1977).

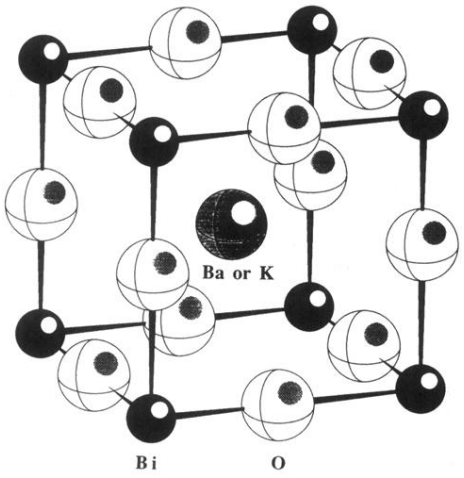

FIG. 1. Crystal structure of the cubic superconductor $Ba_{0.6}K_{0.4}BiO_3$.